

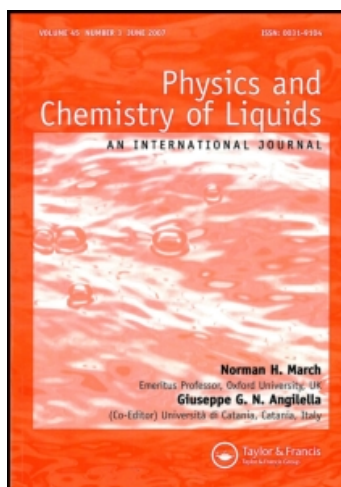
This article was downloaded by:

On: 28 January 2011

Access details: *Access Details: Free Access*

Publisher *Taylor & Francis*

Informa Ltd Registered in England and Wales Registered Number: 1072954 Registered office: Mortimer House, 37-41 Mortimer Street, London W1T 3JH, UK



## Physics and Chemistry of Liquids

Publication details, including instructions for authors and subscription information:

<http://www.informaworld.com/smpp/title~content=t713646857>

### A Test of Computer Simulation of Low Density Gases

J. Ram<sup>ab</sup>; R. Barker<sup>ac</sup>; P. T. Cummings<sup>ad</sup>; P. A. Egelstaff<sup>a</sup>

<sup>a</sup> Physics Department, University of Guelph, Guelph, Ontario, Canada <sup>b</sup> Department of Physics, Banaras Hindu University, Varanasi, India <sup>c</sup> Watershed Energy Systems Ltd., Toronto, Canada <sup>d</sup> Department of Mechanical Engineering, S.U.N.Y. at Stony Brook, Long Island, NY, U.S.A.

**To cite this Article** Ram, J. , Barker, R. , Cummings, P. T. and Egelstaff, P. A.(1982) 'A Test of Computer Simulation of Low Density Gases', *Physics and Chemistry of Liquids*, 11: 4, 315 — 325

**To link to this Article:** DOI: 10.1080/00319108208080753

**URL:** <http://dx.doi.org/10.1080/00319108208080753>

PLEASE SCROLL DOWN FOR ARTICLE

Full terms and conditions of use: <http://www.informaworld.com/terms-and-conditions-of-access.pdf>

This article may be used for research, teaching and private study purposes. Any substantial or systematic reproduction, re-distribution, re-selling, loan or sub-licensing, systematic supply or distribution in any form to anyone is expressly forbidden.

The publisher does not give any warranty express or implied or make any representation that the contents will be complete or accurate or up to date. The accuracy of any instructions, formulae and drug doses should be independently verified with primary sources. The publisher shall not be liable for any loss, actions, claims, proceedings, demand or costs or damages whatsoever or howsoever caused arising directly or indirectly in connection with or arising out of the use of this material.

# A Test of Computer Simulation of Low Density Gases

J. RAM†, R. BARKER‡, P. T. CUMMINGS§, and P. A. EGELSTAFF

*Physics Department, University of Guelph, Guelph, Ontario, Canada N1G2W1*

*(Received October 27, 1981)*

In order to study the pair and three body forces in noble gases it is important to understand the behaviour of the virial series for  $g(r)$  and to have reliable computer simulations of states at low densities. Questions have arisen as to the accuracy of such calculations and in this paper we present new work on this problem for densities near  $1 \times 10^{27}$  atoms/m<sup>3</sup>.

## Introduction

The computer simulation has been used widely to study model fluids.<sup>1</sup> In a canonical NVT ensemble with a small number ( $N$ ) of particles,  $g_N(r)$  will differ from its value for  $N \rightarrow \infty$ . For the limiting case of two particles far apart Lebowitz and Percus<sup>2</sup> have given a correction for finite  $N$ , but when the two particles are close together the size of this correction is unknown.

In addition, for low density gases<sup>3</sup> the mean-free path (m.f.p.) of a particle may be only a few times smaller than the side,  $L$ , of a box containing (say) 500 particles. For example, in the case of hard spheres the mean-free path is related to diameter  $d$  by  $\text{m.f.p.} = d\{\sqrt{2} \cdot \pi\rho^*\}^{-1}$ , where  $\rho^* = \text{density} \times d^3$ . As an estimate for krypton we set  $d =$  the position of the minimum in the pair potential ( $r_m$ ), and data for the range of densities used here are given in Table I. The average number of m.f.p. is about 6, and as the density is reduced a particle may be expected to pass through the box side after a decreasing

---

† On leave of absence from the Department of Physics, Banaras Hindu University, Varanasi-221005, India.

‡ Present address: Watershed Energy Systems Ltd., 108 Liberty St. W., Toronto, Canada.

§ Present address: Department of Mechanical Engineering, S.U.N.Y. at Stony Brook, Stony Brook, Long Island, NY 11794, U.S.A.

TABLE I

Mean-free paths (mfp) and cubical box side (L) as a function of density

$\rho^*$	mfp/ $r_m$	$L/r_m$	Ratio (L/mfp)
0.09007	2.49	17.71	7.1
0.08364	2.69	18.15	6.7
0.07720	2.91	18.64	6.4
0.06434	3.49	19.81	5.7
0.05147	4.37	21.34	4.9

number of collisions. To consider a box where  $L \gg$  m.f.p. we make use of periodic boundary conditions and the effect of this on  $g(r)$  is not clear. It is one of our objectives to see whether a small ratio,  $L/\text{m.f.p.}$ , leads to significant errors.

At low densities  $g(r)$  may be calculated from the virial expansion<sup>4</sup> and it is therefore of interest to compare these and other calculations with Monte Carlo results to try to estimate the size of the above errors. To illustrate our problem we show in Figure 1 an example of  $g(r)$  calculated by the Monte Carlo method (crosses) compared to the expected result for  $\rho \rightarrow 0$  (line). The precision with which the small differences between these two results may be calculated will be investigated in this paper. The study of these small terms is important in the interpretation of experimental data on  $g(r)$  of the kind presented by Teitsma and Egelstaff<sup>5</sup> who used the virial series and Monte Carlo results to interpret their data.

### Virial expansion compared to the Percus–Yevick approximation

The virial expansion for  $g(r)$  in a system of particles interacting with a pair potential,  $u(r)$  is:

$$g(r) = f(r) + 1 + \rho[f(r) + 1] \int f(|\mathbf{r} - \mathbf{s}|)f(s) ds + O(\rho^2) \quad (1)$$

where  $f(r) = [e^{-\beta u(r)} - 1]$  is the Mayer function and  $\beta$  is  $(k_B T)^{-1}$ . The first two terms of this series were calculated using the computer programme VIREXPP; a description of this programme is given in Appendix A. We shall write the virial series in the form:

$$g(r) = \sum_{m=0}^{\infty} \rho^m g_m(r) = e^{-\beta u(r)} \sum_{m=0}^{\infty} \rho^m y_m(r) \quad (2)$$

which defines  $g_m(r)$  and  $y_m(r)$ . If we consider this series cut off at  $m = 1$ , we

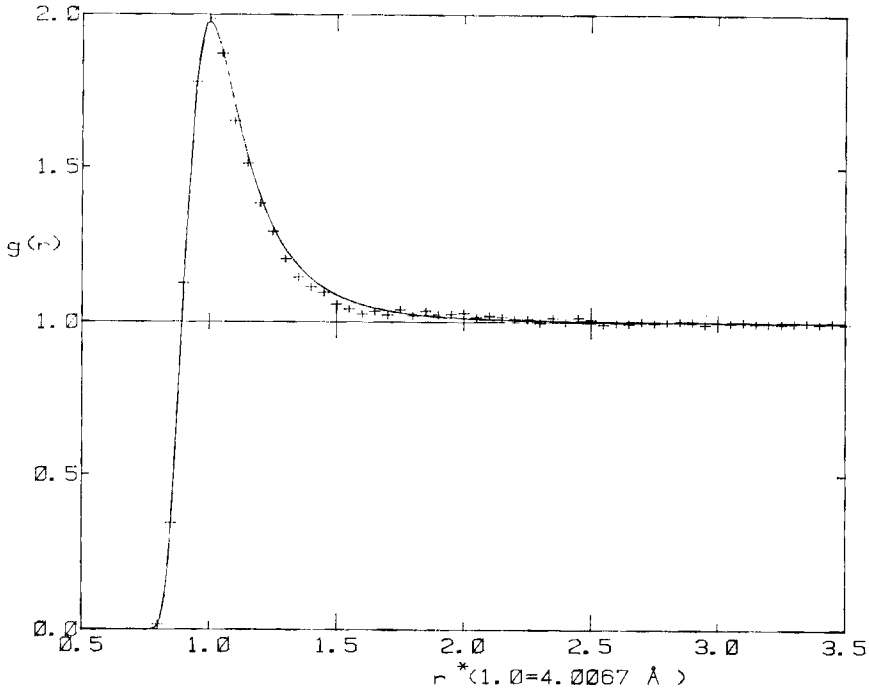


FIGURE 1 Radial distribution function for the Barker *et al.*<sup>7</sup> krypton potentials at  $T = 297$  K and  $\rho = 0.9 \times 10^{27}$  atoms/m<sup>3</sup>. Crosses are Monte Carlo results and the full line is the function  $\exp[-\beta u(r)]$ .

may rewrite Eq. (2) as:

$$y_1(r) \approx \frac{1}{\rho} \left\{ \left[ \frac{g(r)}{g_0(r)} \right] - 1 \right\} = y_1(r) \quad (3)$$

which defines  $y_1(r)$ . Our results are presented in this form in order to amplify the differences between various calculations of  $g(r)$ . We expect that for low enough densities Eq. (2) may be terminated at  $m = 1$  without significant error: in this work we (arbitrarily) set a significance level at 0.2%. In order to estimate the density at which the correction to  $g(r)$  is less than 0.2% we compare our truncated virial data with a calculation using the Percus-Yevick approximation (P.Y.); and we show that the density range considered in this paper meets this condition. It is assumed here that the quantity:

$$\left\{ \sum_{m=2}^{\infty} \rho^m y_m(r) \right\}_{\text{P.Y.}}$$

is nearly equal to the exact value of this sum. This assumption is discussed in Appendix B.

The P.Y. integral equation i.e.:

$$y(r) = 1 + \rho \int \{y(|\mathbf{r} - \mathbf{r}'|)e^{-\beta u(r-r')} - 1\} \{e^{-\beta u(r')} - 1\} y(r') d\mathbf{r}' \quad (4)$$

was solved by an iterative procedure using a grid size of  $0.02 r_m$  and an initial estimate  $y = 1$ . Convergence was enhanced by writing<sup>6</sup>

$$y_{\text{in}}^{(n+1)} = (1 - \alpha)y_{\text{out}}^{(n)} + \alpha y_{\text{out}}^{(n-1)} \quad (5)$$

where  $y_{\text{in}}^{(n)}$  and  $y_{\text{out}}^{(n)}$  are the  $n$ th input and output respectively and  $\alpha$  is a mixing parameter. The iteration was terminated when

$$|y^{(n+1)} - y^n| \leq 0.001$$

For the Barker *et al.*<sup>7</sup> krypton potential we show in Figure 2 the resulting  $g(r)$  in the form of  $y_1(r)$  (full line) at the largest density used here ( $\rho = 1.3 \times 10^{27}$  atoms/ $m^3$  and  $T = 297$  K). For comparison, virial results (truncated at  $m = 1$ ) are plotted as the dashed line. We see that the two results agree to less than 0.2% of the pair correlation function  $g(r)$ , so confirming that the virial expansion is accurate for densities equal to or less than this value.

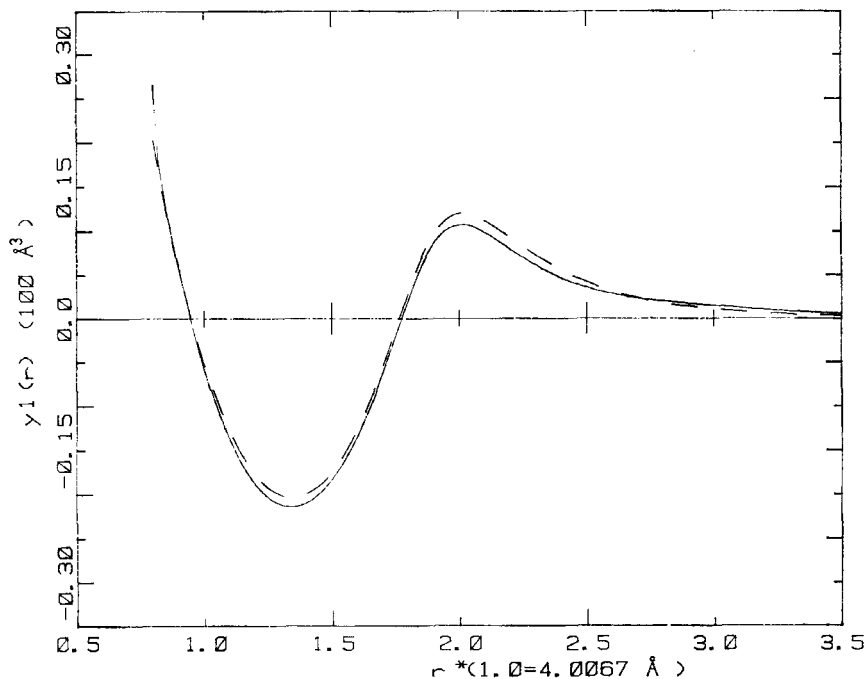


FIGURE 2  $y_1(r)$  from Eq. (3) for  $\rho = 1.3 \times 10^{27}$  atoms  $m^3$  and other parameters as in Figure 1. Full line—P-Y result; dashed line—virial series for  $g(r)$  cut at  $m = 1$ .

### Virial expansion compared to Monte Carlo results

The Monte Carlo calculations using the pair potential were carried out with a 500-particle system located in a cubical box. An NVT ensemble<sup>1</sup> and periodic boundary conditions were used. Five states having densities between 0.8 and  $1.4 \times 10^{27}$  atoms  $m^{-3}$  and a temperature of 297 K were simulated using the pair potentials of Barker *et al.*<sup>7</sup> for krypton (K2) and runs of 500,000 configurations. Each simulation began with the particles being placed randomly with no overlap within the cubical box, and the first 25,000 configurations were used to equilibrate the system. To monitor the calculation for bottlenecks and an insufficient number of equilibrating configurations, the configurational energy and the mean squared displacement were examined every 5000 configurations. After 500,000 configurations, estimates of the average configuration energy and its uncertainty were obtained and compared with the energy obtained from the integral  $\rho/2 \int g(r)u(r) dr$ . The calculation was terminated when two methods gave agreement of (typically) less than 1 percent.

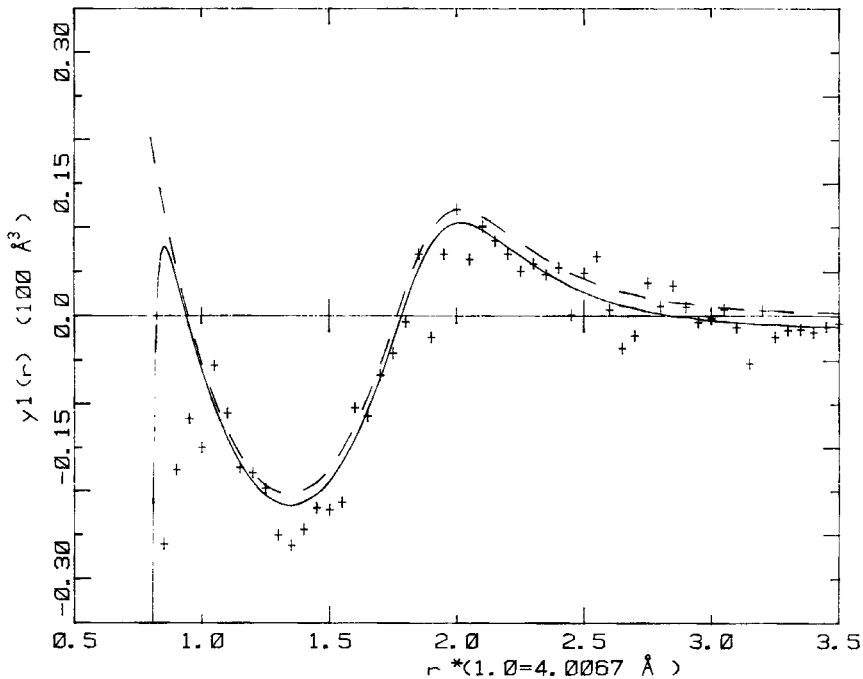


FIGURE 3  $y_1(r)$  from Eq. 3 for  $\rho = 1.3 \times 10^{27}$  atoms/ $m^3$  and other parameters as in Figure 1. Dashed line—virial series for  $g(r)$  cut at  $m = 1$ ; full line shows dashed line plus  $1/N$  correction; crosses—our Monte Carlo results.

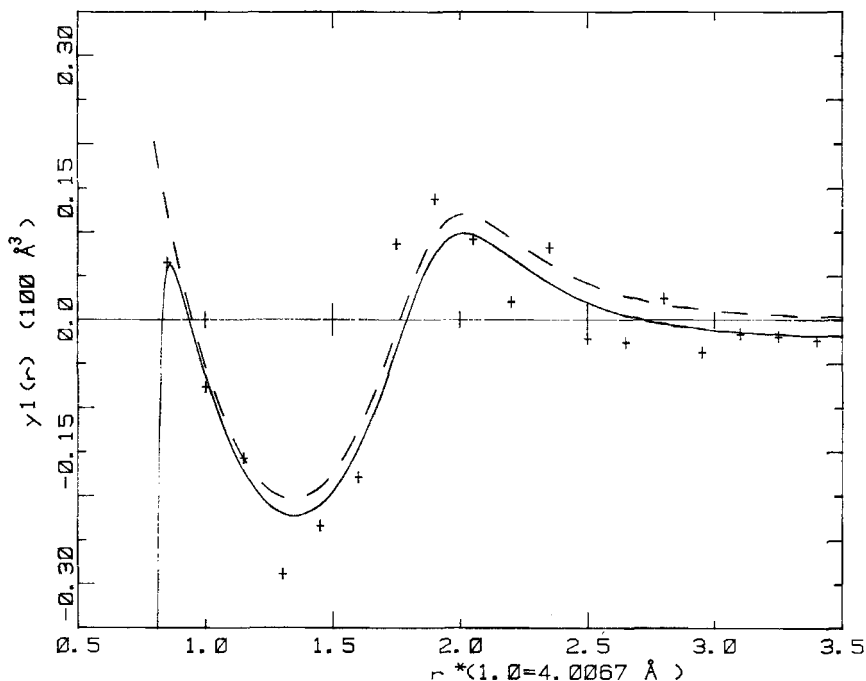


FIGURE 4 Same as in Figure 3 but for  $\rho = 0.9 \times 10^{27}$  atoms/m<sup>3</sup>.

Since the densities are about a factor of ten less than the usual liquid densities, the maximum allowed translation had to be increased to about 3 (in units of  $r_m$ ) to produce a reasonable number of accepted moves. At such low densities the box is mostly empty and to probe the pair potential much larger translations must be allowed. The algorithm in the computer programme that adjusts the maximum allowable translation to produce 50 percent acceptance of the attempted moves worked inefficiently at low densities. For these simulations the ratio of the number of accepted to attempted moves was 0.6 to 0.7.

We found it worthwhile to average the runs at  $\rho = 0.8$  and  $1.0 \times 10^{27}$  atoms/m<sup>3</sup> to improve the statistics and this  $g(r)$  was shown in Figure 1. For the same reason we averaged the runs at  $\rho = 1.2, 1.3$  and  $1.4$  to give a mean at  $\rho = 1.3 \times 10^{27}$  atoms/m<sup>3</sup>. To make a precise comparison we present data for  $y_1(r)$  in Figures 3 and 4. In these figures the crosses are Monte Carlo data and the dashed line shows the result obtained from Eq. (3) using the virial  $g(r)$ . The analogous quantity for a finite number of particles ( $N = 500$ ) is shown by the full line, for which  $g(r)$  in Eq. (3) has been replaced<sup>3</sup> by  $[g(r) - \rho kT\chi_T/N]$  where  $\chi_T$  is the isothermal compressibility.

The value of the compressibility was taken from the virial series. In general there is a discrepancy of the order of 0.2% of  $g(r)$  except where the atoms overlap. The P.Y. result of Figure 2 may be in slightly better agreement with the M.C. data than the virial result.

## Conclusion

The  $1/N$  correction term to  $g(r)$  describes the difference between Monte Carlo and virial results for  $r/r_m > 1.5$  and  $\rho \lesssim 1.3 \times 10^{27}$  atoms/m<sup>3</sup> with room temperature krypton. However for  $r/r_m \sim 1.4$  a discrepancy is seen in both curves which decreases  $y_1(r)$  by about 16%. For a density of  $1 \times 10^{27}$  atoms/m<sup>3</sup> this corresponds to about 0.3% of  $g(r)$ . For small  $r < r_m$  a larger discrepancy is seen in Figure 3 which might be due to the small box size, but further calculations using larger boxes are required to test this conclusion.

We conclude that the interpretation of experimental data through the virial series is reasonably reliable for these densities, and that Monte Carlo calculations at densities of  $\sim 1 \times 10^{27}$  atoms/m<sup>3</sup> are reliable also.

## References

1. J. P. Hansen and J. R. McDonald, *Theory of Simple Liquids* (Academic Press, London, (1976).
2. J. L. Lebowitz and J. K. Percus, *Phys. Rev.*, **122**, 1675 (1961).
3. We consider a dynamical description in terms of the number of mean-free paths, even though we are using a Monte Carlo simulation, partly because of its physical significance and partly because the number of times the particles overlap is significant in M.C. work.
4. S. A. Rice and P. Gray, *Statistical Mechanics of Simple Liquids* (Wiley, New York, 1965).
5. A. Teitsma and P. A. Egelstaff, *Phys. Rev. A.*, **21**, 367 (1980).
6. A. A. Broyles, *J. Chem. Phys.*, **33**, 456 (1960).
7. J. A. Barker, R. O. Watts, J. K. Lee, T. P. Schafer, and Y. T. Lee, *J. Chem. Phys.*, **61**, 3081 (1974).
8. C. Kittel, *Thermal Physics* (Wiley, New York, 1969).
9. L. Verlet and J. J. Weis, *Phys. Rev. A.*, **5**, 939 (1972).
10. S. Labik and A. Malijevisky, *Molec. Phys.*, **42**, 739 (1981).
11. Hard sphere virial results were calculated using expressions from: Hill *Statistical Mechanics*, p. 210 (McGraw-Hill, New York, 1956).
12. L. S. Ornstein and F. Zernike, *Proc. Acad. Sci. Amsterdam*, **17**, 793 (1914).
13. J. A. Barker, R. A. Fisher, and R. O. Watts, *Molec. Phys.*, **21**, 657 (1971).
14. R. A. Aziz and H. H. Chen, *J. Chem. Phys.*, **67**, 5719 (1977).
15. R. A. Aziz, *Molec. Phys.*, **38**, 177 (1979).
16. B. M. Axilrod and E. Teller, *J. Chem. Phys.*, **11**, 299 (1943).
17. P. A. Egelstaff, A. Teitsma, and S. S. Wang, *Phys. Rev. A.*, **22**, 1702 (1980).



## Appendix A

### VIRIAL COEFFICIENT CALCULATIONS

The virial expansion calculations reported in this paper were performed using a programme developed by one of the authors (PTC) building, in part, upon subroutines provided by M. S. Wertheim (unpublished).

The direct correlation function,  $c(r)$ , introduced by Ornstein and Zernike,<sup>12</sup> is related to the structure factor  $S(q)$  in  $q$ -space via the relation

$$S(q) = \frac{1}{1 - \rho c(q)} = 1 + \rho \int (q(r) - 1)e^{iq \cdot r} dr \quad (\text{A.1})$$

where  $c(q)$  is the Fourier transform of  $c(r)$ , and has the following virial expansion

$$c(q) = -2B(q, T) - \rho[3C_1(q, T) + 3C_2(q, T)] \quad (\text{A.2})$$

The integrals  $B(q, T)$ ,  $C_1(q, T)$  and  $C_2(q, T)$  are given by

$$B(q, T) = -\frac{1}{2} \int e^{iq \cdot r} f(r) dr \quad (\text{A.3})$$

$$C_1(q, T) = -\frac{1}{3} \iiint f(r)f(s)f(|\mathbf{r} - \mathbf{s}|)e^{iq \cdot r} dr ds \quad (\text{A.4})$$

$$C_2(q, T) = -\frac{1}{3} \iiint [f(r) + 1][f(s) + 1][f(|\mathbf{r} - \mathbf{s}|) + 1] \\ \times [e^{-u_3(r, s, |\mathbf{r} - \mathbf{s}|)/k_B T} - 1] dr ds \quad (\text{A.5})$$

where  $f$  is the Mayer  $f$ -function and  $u_3$  is the three-body potential. Clearly  $C_2$  is the contribution to the third virial coefficient from the three-body potential.

There is a closely related virial expansion for  $g(r)$ , given in Eq. (2), where the first two terms are given by

$$y_0(r) = 1; \quad y_1(r) = y_{1A}(r) + y_{1NA}(r), \quad (\text{A.6.7})$$

with  $y_{1A}$ ,  $y_{1NA}$  given by

$$y_{1A}(r) = \int f(s)f(|\mathbf{r} - \mathbf{s}|) ds \quad (\text{A.8})$$

$$y_{1NA}(r) = \int [f(s) + 1][f(|\mathbf{r} - \mathbf{s}|) + 1][e^{-u_3(r, s, |\mathbf{r} - \mathbf{s}|)/k_B T} - 1] ds \quad (\text{A.9})$$

This expansion can be easily verified by the reader by noting that

$$S(q) = 1 + \rho h(q) \quad (\text{A.10})$$

where  $h(q)$  is the Fourier transform of  $h(r) = g(r) - 1$ ; combining Eqs. (A.1), (A.2) and (2) yields Eqs. (A.6) to (A.9). The function  $y_1(r)$  is broken up into an additive part,  $y_{1A}(r)$ , due solely to two-body forces, and  $y_{1NA}(r)$ , the contribution to  $y_1(r)$  from the three-body potential.

The program VIREXPP calculates  $B(q, t)$ ,  $C_1(q, T)$ ,  $C_2(q, T)$ ,  $y_{1A}(r)$  and  $y_{1NA}(r)$ , on a user-specified grid of points by writing the integrals in bipolar co-ordinates and using trapezoidal rule quadrature to perform the required numerical integrations. For the users choice of  $f(r)$ , the program dynamically assigns the parameters  $r_{\text{low}}$  and  $r_{\text{max}}$  defined as follows:

$$f(r) = \begin{cases} -1 & 0 < r < r_{\text{low}} \\ e^{-u(r)/k_B T} - 1 & r_{\text{low}} < r < r_{\text{max}} \\ -C_6/r^6 & r > r_{\text{max}} \end{cases} \quad (\text{A.11})$$

The parameter  $C_6$  is the coefficient of  $1/r^6$  in the interaction potential  $u(r)$  and  $C_6/r^6$  is thus the leading term in the large- $r$  behaviour of  $u(r)$  and  $f(r)$ . The parameter  $r_{\text{low}}$  is defined by locating the point at which  $-u(r)/k_B$  becomes too negative for  $e^{-u(r)/k_B T}$  to be defined numerically. The parameter  $r_{\text{max}}$  has been determined empirically by requiring that the calculated results be independent of  $r_{\text{max}}$ . In calculating  $B(q, T)$ , a series expansion is used to calculate that part of the integral in Eq. (A.3) over the range  $t > r_{\text{max}}$ . Integrals in Eq. (A.4) and (A.5) are simply truncated at  $r_{\text{max}}$ . As a time-saving device, different values of  $r_{\text{max}}$  and different trapezoidal grid widths are used in calculating each of  $B(q, T)$ ,  $C_1(q, T)$  and  $C_2(q, T)$ ; in the latter case, the long-ranged nature of the integral requires a relatively large  $r_{\text{max}}$ .

This program allows the user to select from a range of model potentials (such as those of Barker *et al.*,<sup>7,13</sup> Aziz and co-workers,<sup>14,15</sup> and the Axilrod-Teller triple-dipole three-body potentials).<sup>16</sup> For the results presented in this paper, only  $y_{1A}(r)$  and  $g_n(r) = e^{-u(r)/k_B T} y_n(r)$ ,  $n = 0, 1$ , for one model potential are required. Results obtained using the other capabilities of VIREXPP have been reported elsewhere.<sup>17</sup>

## Appendix B

### PRECISION OF THE P.Y. APPROXIMATION AT LOW DENSITIES

We have used results obtained in the P.Y. approximation as essentially exact results at low densities. For terms  $O(\rho^2)$  in  $g(r)$  there could be small corrections at contact and at two or three atomic diameters. In the former case we

tested for the size of these corrections by comparing P.Y. results for the hard sphere fluid with the semi-empirical formula of Verlet and Weis.<sup>9</sup> The agreement was found to be much better than our significance level because the Verlet–Weis correction is very small at our low densities. The Verlet–Weis results are also in excellent agreement with the recent Monte Carlo hard sphere simulation data<sup>10</sup> at the lowest density given ( $\rho d^3 = 0.3$ ). This comparison is shown in Figure 5. The agreement in this figure is better than in any of our other figures. Thus the correction at contact is unimportant, and we assume that this implies that the contribution from the diagrams omitted in the P.Y. expansion in the case of a real potential is unimportant.

If this is so we would expect the virial results<sup>11</sup> for hard spheres of diameter  $d$  to show differences from the Verlet–Weiss results of about the same size as those illustrated for a real potential in Figure 2. Such a comparison for  $\rho d^3 = 0.09007$  is given in Figure 6, with results as expected.

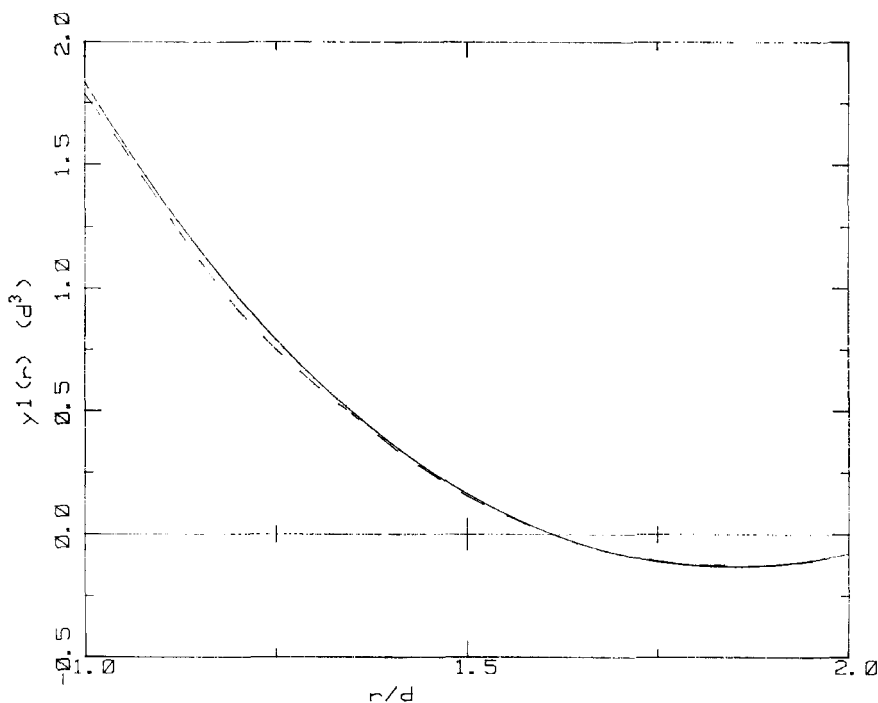


FIGURE 5  $y_1(r)$  for hard sphere Monte Carlo data<sup>10</sup> and the Verlet–Weis formula<sup>9</sup> for  $\rho d^3 = 0.30$ . VW—full line; MC—dashed line.

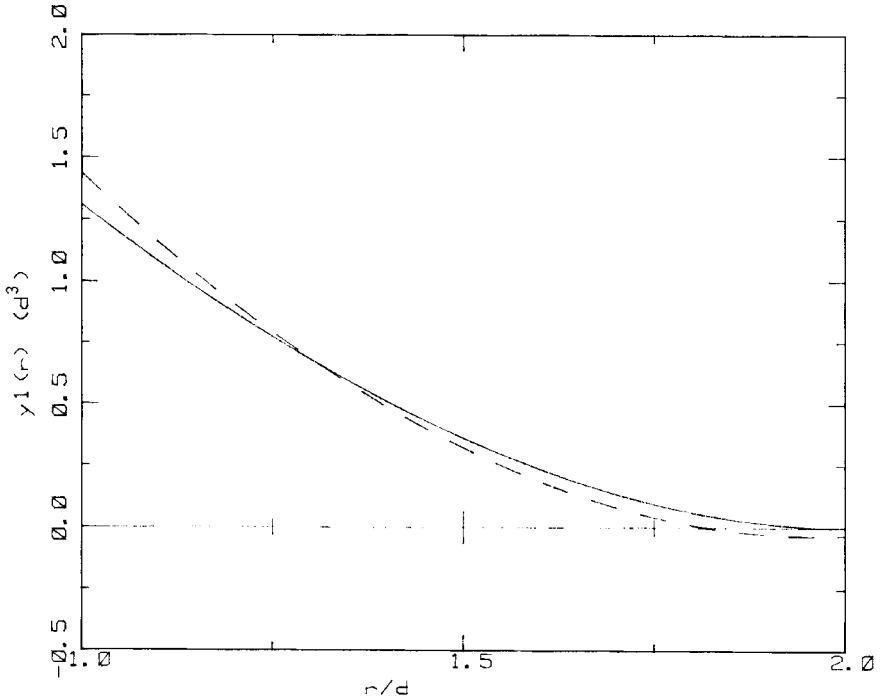


FIGURE 6  $y_1(r)$  for hard spheres at  $\rho d^3 = 0.09007$ . The full line is calculated from the virial expansion for  $g(r)$  cut at  $m = 1$ , and the dashed line is the Verlet-Weiss<sup>9</sup> result.